FLUCOME 2009
10th International Conference on Fluid Control, Measurements, and Visualization
August 17–21, 2009, Moscow, Russia

UNSTEADY SURFACE PRESSURE MEASUREMENTS ON A HEMISPHERICAL DOME WITH PRESSURE-SENSITIVE PAINT

Shuo Fang[1], Kevin J. Disotell[2], James W. Gregory[3],
Frank C. Semmelmayer[4], and Robert W. Guyton[5]

ABSTRACT

Porous pressure-sensitive paint (PSP) is used in this work to measure the global, unsteady surface pressure distribution on a hemispherical dome at several flow conditions in the United States Air Force Research Laboratory's Trisonic Gasdynamics Facility. This investigation is part of a larger study into the fundamental dynamics and control of unsteady separated shear layers on hemispherical domes. The present work focuses on the development and implementation of fast-responding polymer/ceramic PSP for measurement of unsteady surface pressures in a large-scale wind tunnel environment. Phase-averaged unsteady PSP data at two subsonic freestream conditions are presented and compared with data from pressure taps mounted along the centerline of the dome. Unsteady test conditions were Mach 0.3 and 0.6 at a total pressure of 24 kPa, where the predominant shear layer frequencies were 266 and 281 Hz, respectively. The required hardware and software configurations are described, including the phase-locking and light intensity monitoring techniques utilized.

Keywords: Porous Pressure-Sensitive Paint, Unsteady, Hemispherical Dome

INTRODUCTION

Pressure-Sensitive Paint

Pressure-sensitive paint (PSP) is an optical measurement technique which provides global surface pressure data to the experimenter. Compared to traditional pressure measurement techniques, such as arrays of pressure taps installed on a test model, PSP provides non-intrusive global pressure mapping with very fine spatial resolution. Extensive reviews of PSP have been written by Liu *et al.* (1997) and Bell *et al.* (2001).

PSP is based on the luminescence of oxygen-sensing molecules, known as luminophore, which are dispersed in a permeable paint binder. A short-wavelength light source is used to excite the luminescent molecules to a higher energy state, causing longer-wavelength light to be emitted from the excited molecules through radioactive decay. This property of luminescence is known as the Stokes shift. The intensity of the light emission is influenced by the process of oxygen quenching,

[1] Department of Aerospace Engineering, The Ohio State University, e-mail: Fang.89@osu.edu
[2] Department of Aerospace Engineering, The Ohio State University, e-mail: Disotell.1@osu.edu
[3] Corresponding author: Department of Aerospace Engineering, The Ohio State University, e-mail: Gregory.234@osu.edu
[4] Aircraft Integration Branch, Air Vehicles Directorate, United States Air Force Research Laboratory, Wright-Patterson AFB, e-mail: Frank.Semmelmayer@WPAFB.AF.MIL
[5] Aircraft Integration Branch, Air Vehicles Directorate, United States Air Force Research Laboratory, Wright-Patterson AFB, e-mail: Robert.Guyton2@WPAFB.AF.MIL

which causes a decrease in the luminescent intensity as the concentration of oxygen molecules (air pressure) increases. The measured light intensity can be converted to pressure in one of several ways. For this study, an intensity-based method is employed, where the pressure is derived from a ratio of wind-on and wind-off images. The wind-off image captures the reference conditions of the test, while the wind-on image is taken with air flowing over the painted surface of interest. The two images must be perfectly aligned in order to extract accurate pressure data, otherwise significant noise will be introduced as false pressures. A process of image registration can be used to align the wind-off and wind-on images to within acceptable error. Bell *et al.* (1996) stipulate that registration error should ideally be less than half a pixel. Furthermore, false pressure data can be introduced if the intensity of excitation light varies from image to image; it is desirable for the excitation light level to remain constant.

The rate at which the oxygen quenching process occurs is directly related to the response time of the paint. The response time of PSP is governed by two parameters, paint thickness and the diffusion coefficient of the binder material, which are related by

$$\tau_{diff} \propto \frac{h^2}{D_m} \tag{1}$$

where τ_{diff} is the response time, h is the binder thickness, and D_m is the diffusion coefficient of the binder. This indicates that the time response of PSP can be increased by either decreasing the binder thickness or by increasing the diffusivity of the binder. Both cases have been studied extensively in the effort to produce a fast-responding PSP formulation that outperforms conventional polymer-based paints.

A formulation known as porous PSP has recently been developed with the philosophy of increasing oxygen diffusivity within the binder layer. A schematic comparison between the oxygen quenching process of conventional polymer-based PSP and porous PSP is shown in Figure 1 provided by Sakaue (1999). For oxygen quenching to take place in conventional polymer-based PSP, oxygen molecules must permeate into the binder before they can interact with the luminescent molecules, causing a delay in the response. In contrast, the porous binder allows the luminescent molecules to be more "open" to the test gas so that they can interact freely with the oxygen molecules, increasing the response time dramatically. Extensive information on the chemistry, applications, and data reduction techniques of polymer-based and porous PSP is presented in the text by Liu and Sullivan (2005) and the review by Gregory *et al*. (2008).

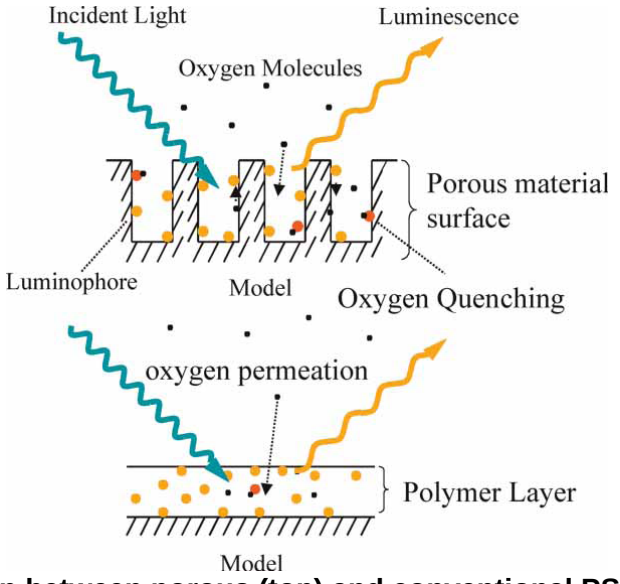

Fig. 1. Comparison between porous (top) and conventional PSP (Sakaue, 1999).

Although an abundance of conventional steady PSP tests have been conducted, only a handful of unsteady test cases have been reported. Several unsteady PSP experiments are reviewed by Gregory *et al.* (2008). Klein *et al.* (1999) reported unsteady PSP results of a 65° delta wing, rotating periodically at 10 Hz, using the phase-locking technique. Gregory *et al.* (2002) reported dynamic calibration results of several PSP formulations using a fluidic oscillator. The results showed that the frequency response of polymer/ceramic PSP (PC-PSP), which is classified as a porous paint, was at least 20 kHz. Gregory (2004) had also reported on the application of polymer-ceramic PSP for measuring the unsteady surface pressures in turbomachinery, where the PC-PSP was able to resolve surface pressure fluctuations at a blade passage frequency of 1.67 kHz.

To demonstrate the capability of porous PSP in resolving unsteady flow features on a wind tunnel model, it is applied to a hemispherical dome in subsonic flow and compared to the data collected from the pressure taps and unsteady pressure transducers mounted along the centerline of the dome. This type of flow field is complex, as reported by Vukasinovic *et al.* (2005), who studied the flow over a surface-mounted hemispherical shell mounted in a wind tunnel, using PIV methods, at Reynolds numbers up to 700,000. The present study is particularly important in the development of aero-optical systems, where knowledge of the surface pressure fluctuations can influence the design of bluff bodies which require minimum optical distortions through the separated shear layer.

EXPERIMENTAL SETUP

Hemispherical Dome

The hemispherical dome used in these experiments, shown in Fig. 2(a), was provided by the United States Air Force Research Laboratory. The dome measures approximately 300 mm in diameter and is primarily composed of a polymer material, with a small metallic disk located on the top. An array of 12 pressure taps were placed along the centerline of the dome for performing an *in situ* calibration of the PSP, as well as to compare the pressure data measured by pressure transducers. Two Kulite pressure transducers were installed just behind the center of the dome to obtain the reference signal of the unsteady separated shear layer. Figure 2(b) provides a schematic representation of the locations for the pressure taps, represented by the circles, and Kulite transducers, represented by the solid squares. The blue arrow marks the differential pressure transducer, and the green arrow marks the absolute pressure transducer.

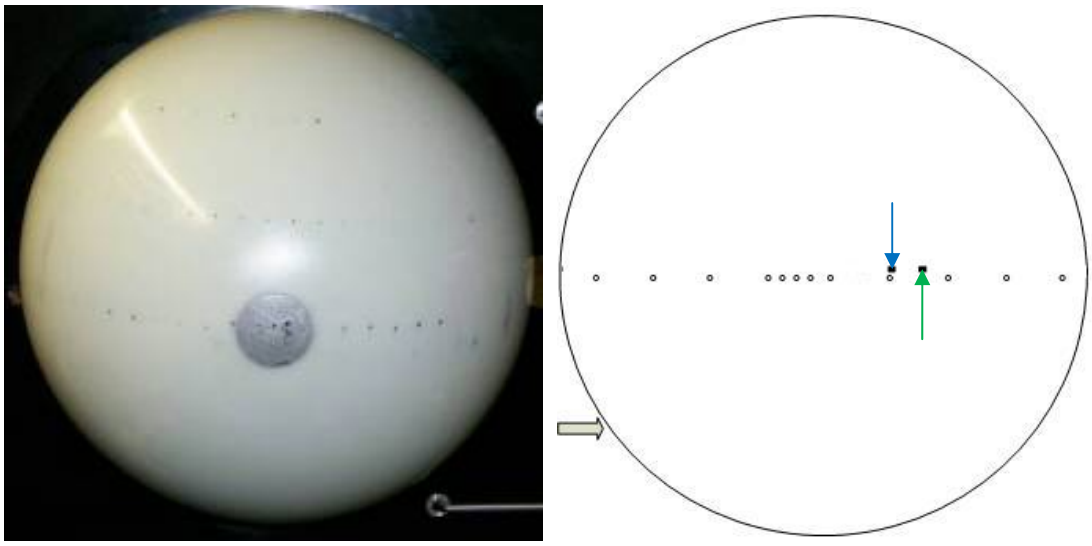

(a) **(b)**

Fig. 2. (a) Test model and (b) pressure tap and Kulite transducer locations.

The unsteady pressure signal was acquired digitally from the Kulite pressure transducers using a National Instruments SCXI-1000 signal conditioner and data acquisition unit. The calibrated

pressure signals from both Kulite pressure transducers for Mach 0.3 and Mach 0.6 are shown in Figure 3. The M=0.3 case has RMS fluctuations of 0.2 kPa for the differential pressure transducer, and 0.13 kPa for the absolute transducer. The M=0.6 case has RMS fluctuations of 0.85 kPa for the differential transducer, and 0.88 kPa for the absolute transducer.

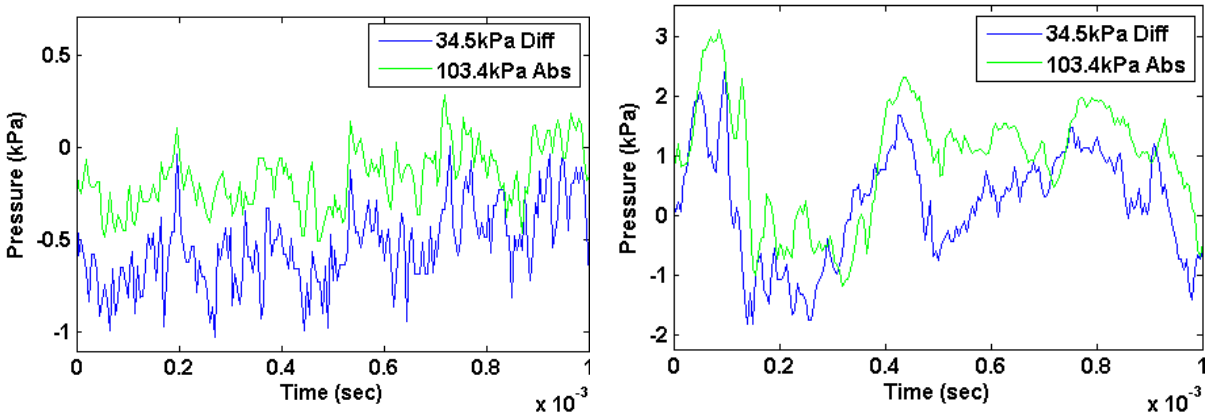

Fig. 3. Normalized Kulite pressure data at (a) M=0.3 and (b) M=0.6.

The power spectra generated from the raw pressure transducer data for the Mach 0.3 and 0.6 test cases are shown in Figure 4. At Mach 0.6, the fundamental frequency of the separated shear layer was approximately 281 Hz. At Mach 0.3, two frequency peaks were present, at 266 Hz and 530 Hz. Only the 266 Hz frequency peak was used for phase-locking of the PSP data.

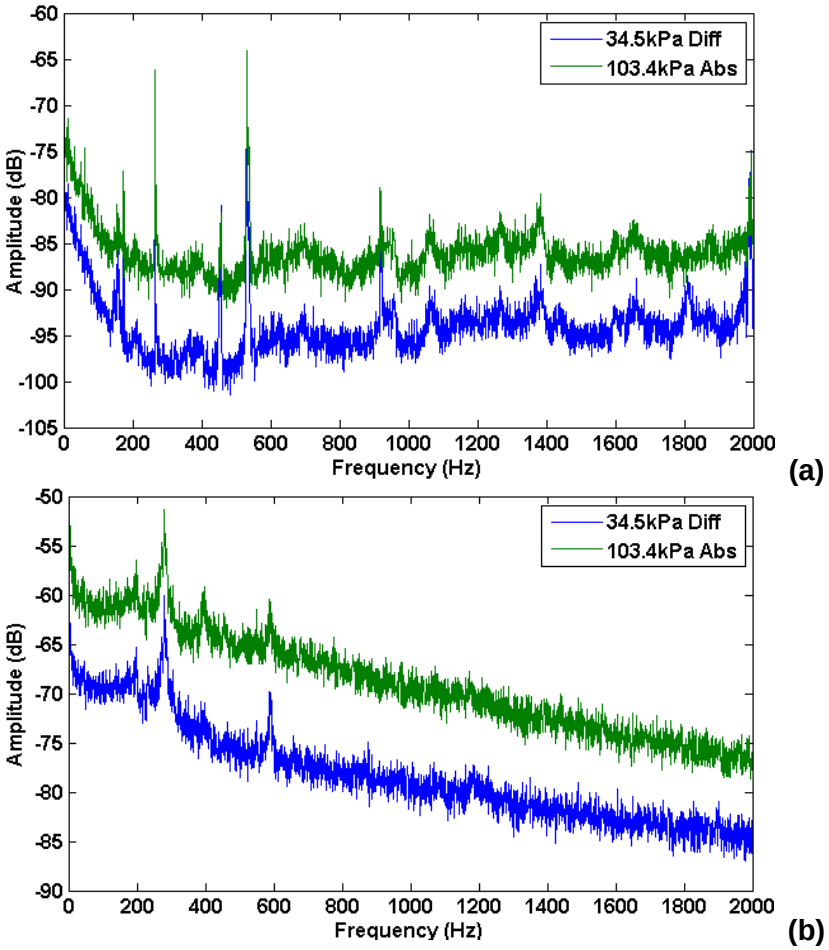

Fig. 4. Power spectra for (a) M=0.3 and (b) M=0.6.

Instrumentation

The hemispherical dome was painted with a porous polymer-ceramic binder layer and over-sprayed with bathophen ruthenium complex as the luminophore using an airbrush. The dome was then installed on a splitter plate in the Trisonic Gasdynamics Facility tunnel at the United States Air Force Research Laboratory. Two sets of CCD cameras and LED arrays, shown in Figure 5, were used to image the forward and aft regions of the hemisphere.

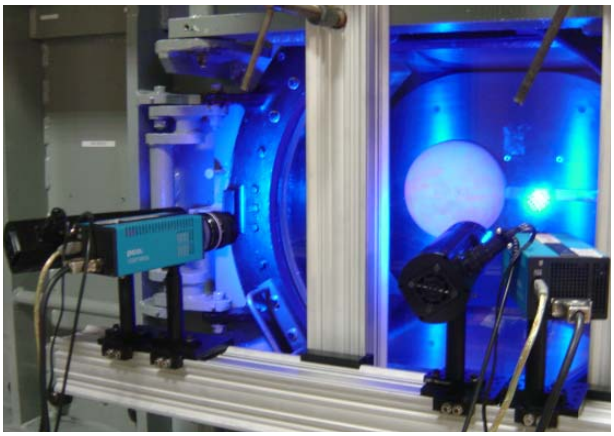

Fig. 5. Mounting arrangement for CCD cameras and LEDs.

The blue LED lights were used to excite the luminophore molecules. The emitted light from the molecules was captured by two 14-bit Cooke Corp. CCD cameras, each with 1200x1600-pixel resolution. A 590-nm long-pass optical filter was placed in front of the camera lens to filter out the excitation light, allowing only the emitted light to be captured.

Since an intensity ratio between the wind-on and wind-off images must be obtained to acquire the pressure data, the two images must be aligned to avoid noise corruption. During operation of the wind tunnel, the vibration of the side walls posed a threat to proper alignment of the cameras. By securing the CCD cameras and LED units to the wind tunnel with three aluminum trusses, C-clamps, and mounting brackets, the cameras were able to shift with the wind tunnel when capturing the two images. This rendered the misalignments between the two images negligible.

Unsteady PSP Measurements

The configuration for obtaining unsteady measurements is shown in Figure 6. The signals from the Kulite pressure transducers were conditioned with a National Instruments SCXI-1000 Chassis with one 1140 module and two 1121 modules installed, and digitized with a PCIe-6251 DAQ board. The analog transducer signals were simultaneously monitored real-time on an oscilloscope after being amplified and filtered using a fourth-order Butterworth band-pass filter (Krohn-Hite Model 3364). In order to capture the pressure characteristics in one instant of the oscillation cycle, the LED lights were required to pulse at the same frequency as the shear layer fluctuations. Thus, the excitation from LED arrays was phase-locked to the predominant shear layer frequency measured by the pressure transducers. This was accomplished by triggering off a particular point on the amplified and filtered transducer signal waveform with an oscilloscope (Agilent DSO5034A). The oscilloscope generated a pulse for every trigger event, which was subsequently used to trigger a digital pulse/delay generator (Berkeley Nucleonics Model 575). The pulse/delay generator was used to drive the LED units with a variable delay set to step through 20 equal increments throughout the mean period. The camera shutter was held open for a long period to integrate a sufficient amount of light to reach near full-well capacity. A camera shutter status signal was used to gate the pulse signal to the LED units, such that the luminescent molecules were only excited when the camera shutter was open, to reduce the effects of photo-degradation. To measure the total intensity of light emitted by the LED units, a pulse counter (National Instruments PCI-6602) was used to monitor the number of pulses sent to the light sources.

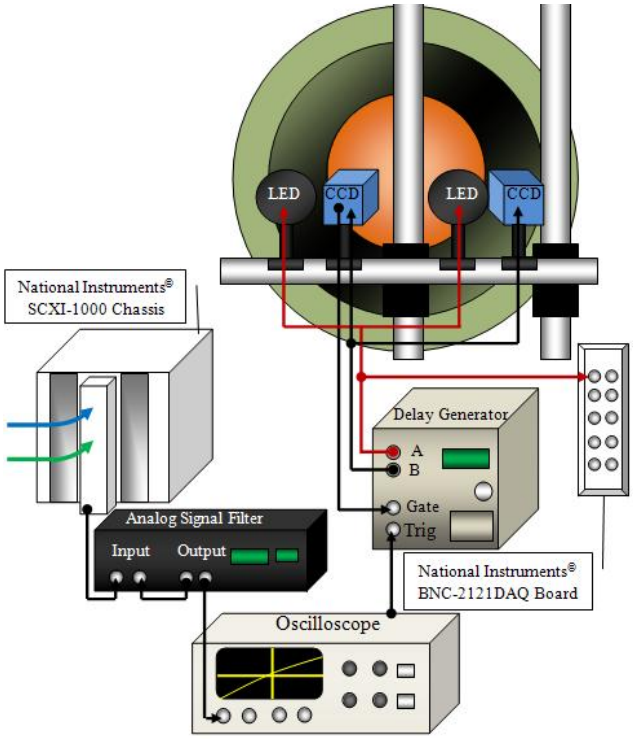

Fig. 6. Setup for unsteady pressure measurements.

For both the M=0.3 and M=0.6 test cases, phase-averaged unsteady data were collected by setting the camera to capture and average 32 images with an exposure time of 250 ms. For the M=0.3 case, the oscilloscope hold-off time was set to 4.72 ms to allow sufficient time for the oscilloscope to re-arm and create the next pulse; similarly, a hold-off time of 5 ms was set for the M=0.6 case. A total of 20 delay steps were used, with each delay step taken as 5% of the oscillation period.

Data Reduction

The full-field images acquired from the CCD cameras were used to obtain the intensity ratio by dividing the wind-off reference image by the phase-averaged wind-on images. The pressure signals were converted to a pressure ratio by dividing the static pressure by the total pressure. An *in situ* calibration was performed by fitting the relationship between the intensity ratio and the pressure ratio to a first-order polynomial. The calibration was applied to the intensity ratio to obtain a pressure ratio, which was then multiplied by the total pressure to obtain the static pressure value in kPa.

RESULTS

The unsteady PSP results for the M=0.3 and M=0.6 cases are presented below. Only data collected from the camera with the viewing angle tilted such that the upstream stagnation point is visible, leaving a portion of the downstream side of the model out of view, will be considered. Therefore, some pressure tap data in the aft portion of the test model has been omitted. A circular-shaped intensity change was observed for all test cases, which is believed to have been caused by the circular aluminum disk located at the top of the dome shown in Fig. 2(a). Since a change in substrate material would cause a change in the surface temperature in that region, the PSP (which is also temperature sensitive) would certainly react to this temperature change with a noticeably different light emission signature. Therefore, the circular shape can be disregarded from the rest of the data.

It was observed that the intensity of the LED arrays varied from image to image, particularly at delay steps greater than half of the period. The pulse counter used to monitor the trigger signals sent

to the LED arrays showed that the number of pulses remained relatively constant from image to image, which was interpreted to mean that the light level remained constant throughout the sequence. However, the reduced data showed a drop-off in light intensity as the delay increment was increased over the second half of the period. This observation points to a hardware issue which is currently being investigated.

Mach 0.3 Unsteady Data

Unsteady PSP data for the M=0.3 case, with zero delay, is shown in Fig. 7. From figure, the stagnation point at the leading edge has the highest pressure as the flow expands rapidly around the surface. The pressure decreases gradually, and reaches its minimum at a location on the hemisphere of approximately 100°. Flow separation could be seen further downstream on the dome, where an adverse pressure gradient forms. Due to the three-dimensional geometry of the test model, which is curvilinear in both the streamwise and spanwise directions, the spanwise pressure profile is subjected to distortions that make the separation line appear to have a horseshoe shape.

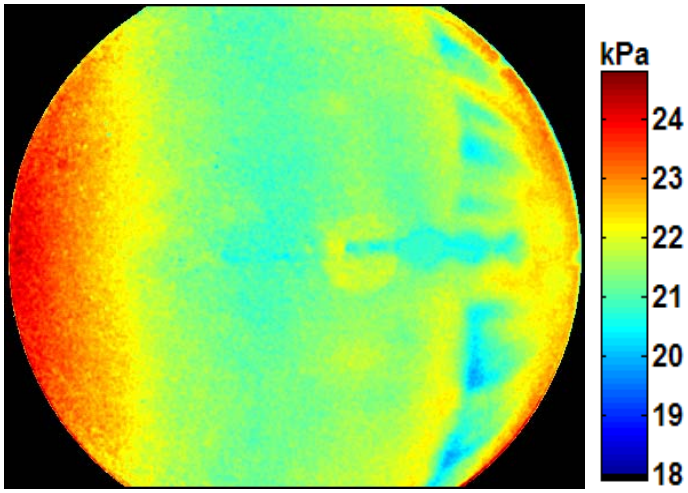

Fig. 7. Unsteady PSP data at M=0.3 (P_0=24 kPa).

Fig. 8 shows a comparison between the PSP data and the pressure tap data at different angular positions, with respect to the mounting surface, on the hemisphere. Note that the pressure spike between the 80º and 100º positions is caused by the aluminum plate located on top of the model. The two measurement techniques appear to correlate very well near the leading edge of the hemisphere, but past the 100º location, the PSP data appear to resolve finer pressure variations in the flow that was not captured by the pressure taps.

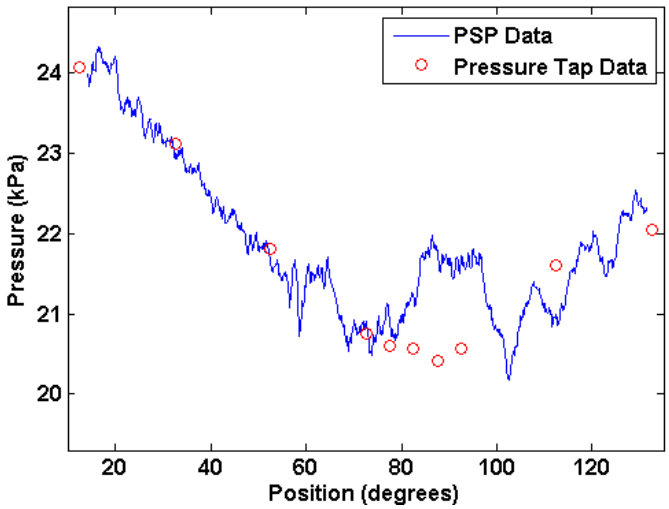

Fig. 8. Unsteady PSP and pressure tap data at M=0.3 (P_0=24 kPa).

Full-Field Unsteady Data

For the M=0.3 case, the oscillation period was 3.76 ms. The delay generator was used to generate 20 phase delays, in increments of 188 μs, which represent 5% of the period. The sequence of images shown in Fig. 9 represents four of the 20 equally-spaced unsteady pressure data, throughout one period in the oscillation, where τ represents the time instance in the oscillation, and T represents the period. These images were used to generate a short video clip to visualize the pressure variations within one period of the oscillation.

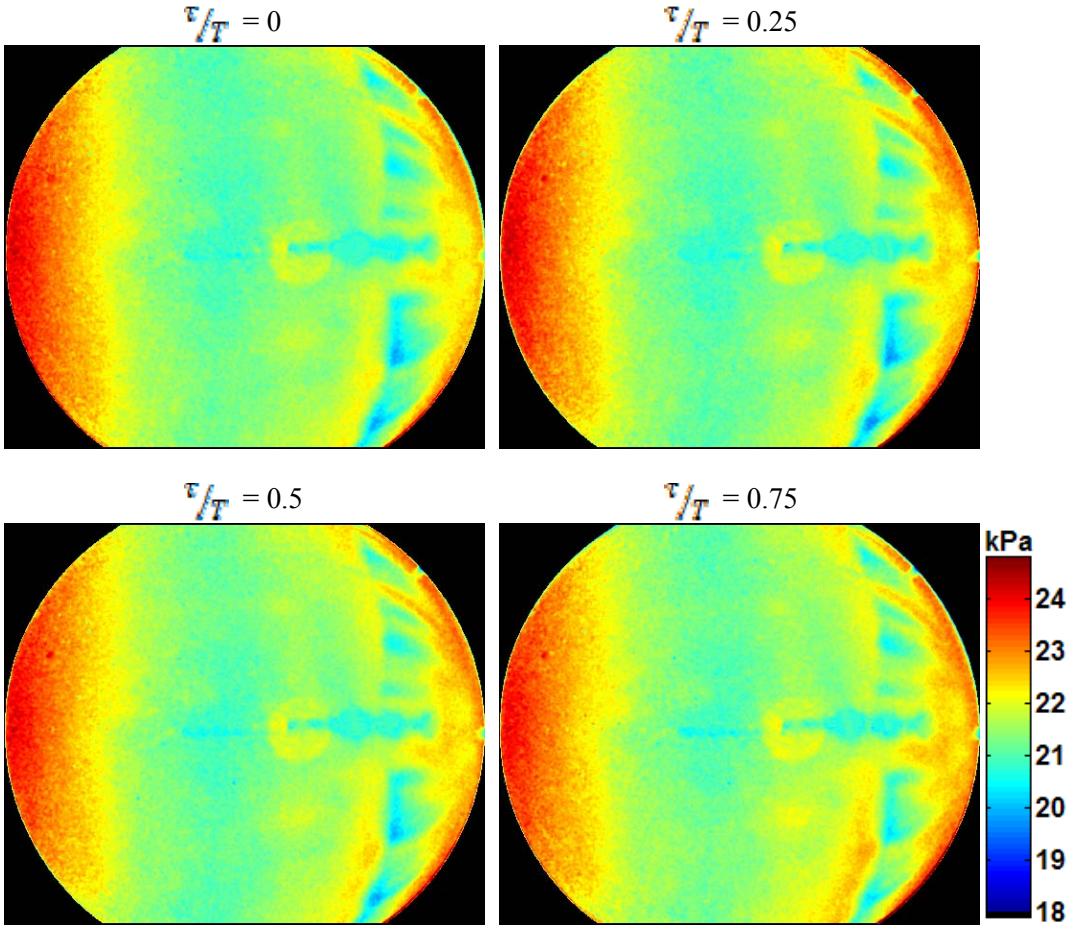

Fig. 9. Full-field PSP data for M=0.3 (P_0=24 kPa) at various points in the oscillation.

Fig. 10 shows cross-sectional plots of the PSP data, taken along a profile about 20 mm below the center line, that best show the separation location. The plots represent the four different instances in the oscillation cycle corresponding to the images in Fig. 9. From this plot, small fluctuations can be observed in the location of the separation line.

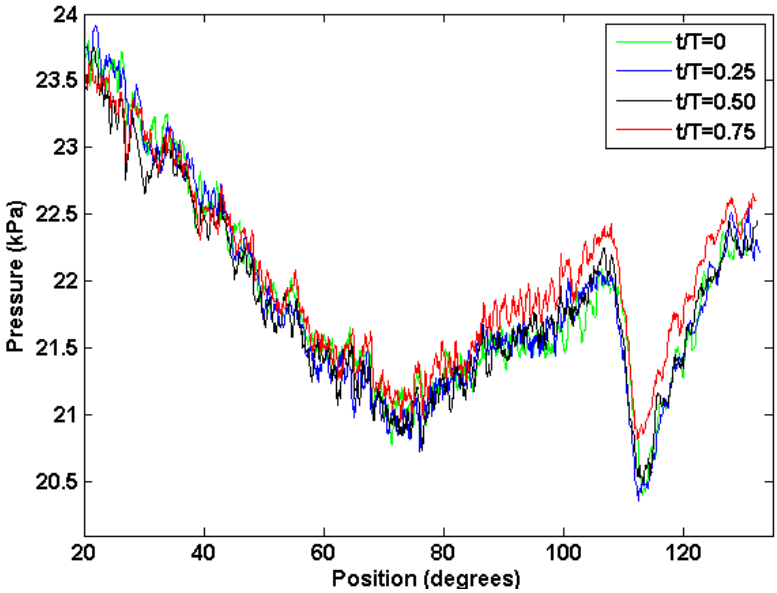

Fig. 10. Cross-sectional plots of unsteady PSP measurements at M=0.3 (P_0=24 kPa).

Mach 0.6 Unsteady Data

The unsteady PSP data for the M=0.6 case is shown in Fig. 11. From the figure, a shock is clearly visible at the 85º location. Like the M=0.3 case, the three-dimensional geometry of the test model causes the shock to take on a horseshoe appearance. A very interesting phenomenon can be seen just behind the shock, which appears to be a type of three-dimensional shock interaction. Further study will be conducted on this observed phenomenon.

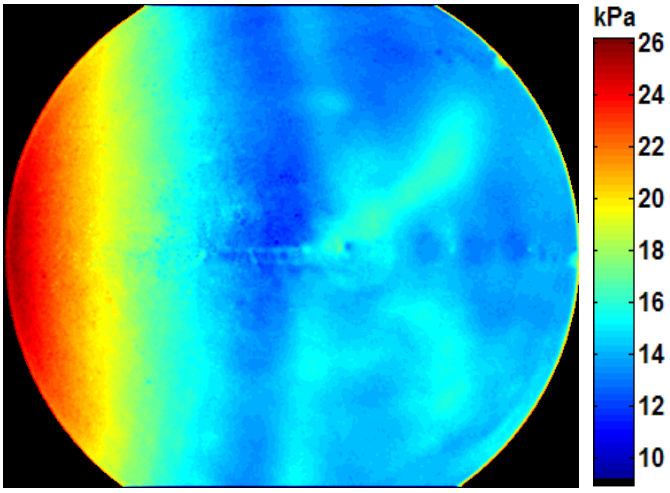

Fig. 11. Unsteady PSP data at M=0.6 (P_0=24 kPa).

Fig. 12 shows a comparison between the PSP data and the pressure tap data at different angular positions, with respect to the mounting surface, on the hemisphere. The PSP profile appears to correlate very well with the pressure tap data at the front section of the model, but deviates further near the aft section of the model mainly due to the viewing angle, where not as much of the intensity is captured, and due to the temperature effects of the metal disk near the center of the model.

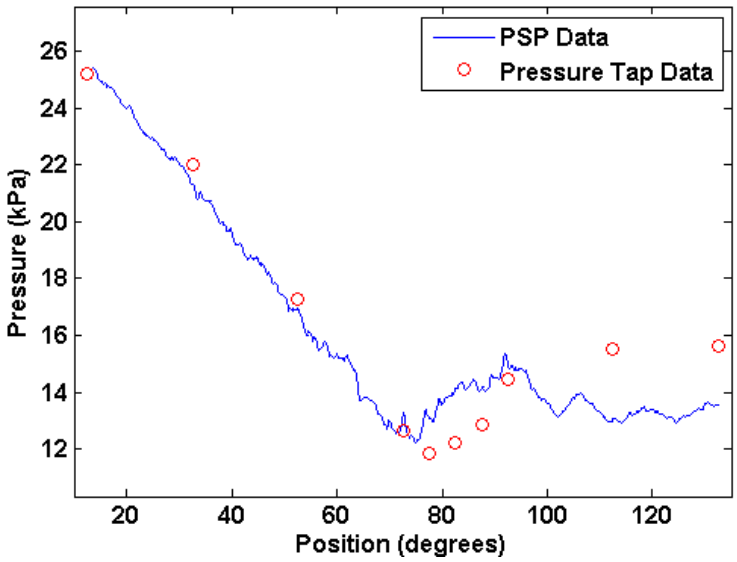

Fig. 12. Unsteady PSP and pressure tap data at M=0.6 (P_0=24 kPa).

Full-Field Unsteady Data

For the M=0.6 case, the oscillation period was 3.56 ms. The delay generator was used to generate 20 phase delays, in increments of 178 μs, which represent steps of 5% of the period. The sequence of images shown in Fig. 13 represents 4 of the 20 equally-spaced unsteady pressure data, throughout one period in the oscillation, where τ represents the instance in the oscillation, and T represents the period.

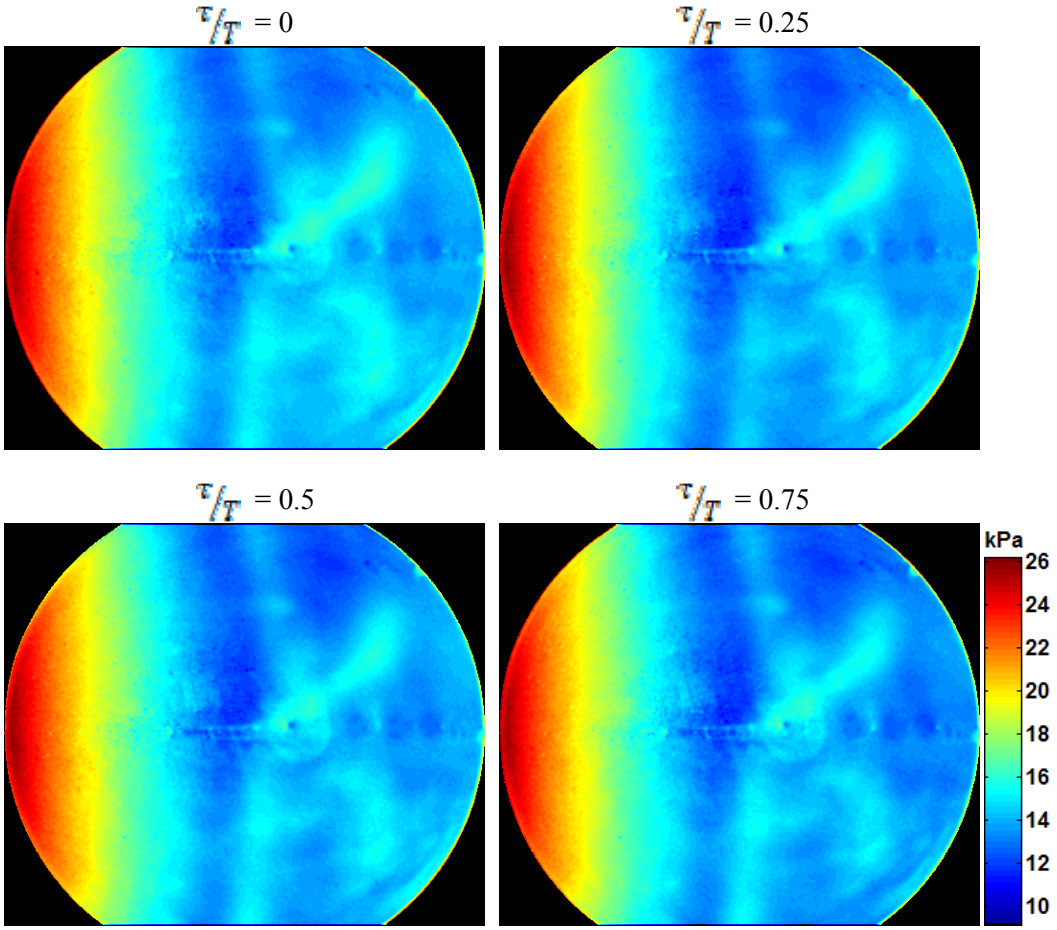

Fig. 13. Full-field PSP data for M=0.6 (P_0=24 kPa) at various points in the oscillation.

Fig. 14 shows a cross-sectional plot of the PSP data, along a profile just below the location of the pressure taps to minimize any distortions in the flowfield caused by the pressure taps. The profiles represent four equally-spaced instances in the oscillation cycle, correlating to the images presented in Fig. 13. As expected, the pressure variations on the upstream side of the flow remains mostly constant, but pressure variations increases further down the flow, especially around the area where the 3-dimensional shock interaction occurs.

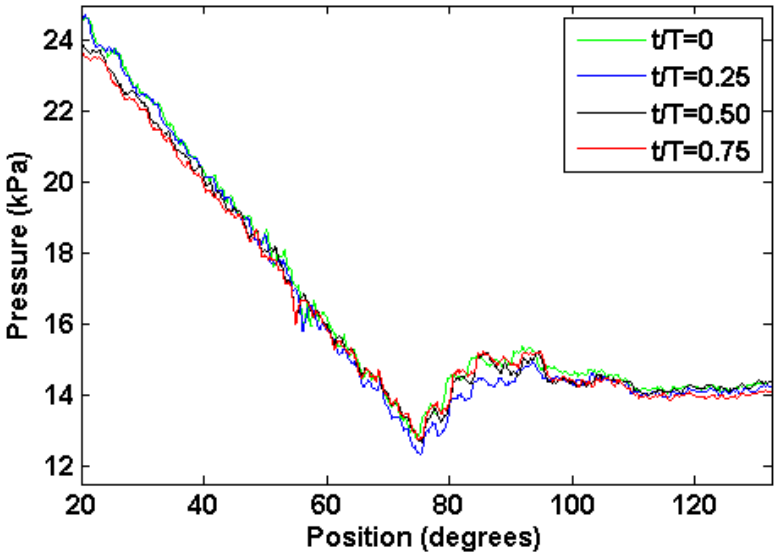

Fig. 14. Cross-sectional plots of unsteady PSP measurements at M=0.6 (P_0=24 kPa).

CONCLUSIONS

For this experiment, the porous pressure-sensitive paint technique was successfully applied to an unsteady test on a large-scale wind tunnel model. Global, unsteady surface pressure measurements on a hemispherical dome in Mach 0.3 and Mach 0.6 flow were successfully resolved with very fine spatial resolution, revealing evidence of a three-dimensional shock structure on the aft portion of the model. The polymer/ceramic PSP proved to be an effective tool for studying unsteady pressure flow fields with shear layer frequencies of 266 Hz and 281 Hz at Mach 0.3 and Mach 0.6, respectively. Furthermore, the PSP data correlated well with the pressure tap and transducer data on the forward portion of the hemisphere. A pulse counter was used to monitor the trigger signals sent to the LED arrays, but while the number of pulse counts was observed to remain relatively constant, the light level continued to vary from image to image. Future work will focus on improving the uniformity of light over the surface of the model, either through modification of the existing hardware configuration or the development of an appropriate correction scheme.

ACKNOWLEDGMENTS

The authors gratefully acknowledge the Air Vehicles Directorate at the United States Air Force Research Laboratory for providing the funding and facility time for this work.

REFERENCES

Bell, J.H. and B.G. McLachlan (1996), "Image Registration for Pressure-Sensitive Paint Applications," *Experiments in Fluids*, **22**(1), 78-86.

Bell, J.H., E.T. Schairer, L.A. Hand, and R.D. Mehta (2001), "Surface Pressure Measurements Using Luminescent Coatings," *Annual Review of Fluid Mechanics*, **33**, 155-206.

Gregory, J.W. (2004), "Porous Pressure-Sensitive Paint for Measurement of Unsteady Pressures in Turbomachinery," 42nd AIAA Aerospace Sciences Meeting (AIAA 2004-0294), Reno, NV.

Gregory, J.W., H. Sakaue, and J.P. Sullivan (2002), "Fluidic Oscillator as a Dynamic Calibration Tool," 22nd Aerodynamic Measurement Technology and Ground Testing Conference (AIAA 2002-2701), St. Louis, MO.

Gregory, J.W., K. Asai, M. Kameda, T. Liu, and J.P. Sullivan (2008) "A review of pressure-sensitive paint for high-speed and unsteady aerodynamics," *Proceedings of the Institution of Mechanical Engineers, Part G: Journal of Aerospace Engineering*, **222**(2), 249-290.

Klein, C. and R.H. Engler (1999), "Visualization of Aerodynamic Effects on a Double-delta Wing Aircraft Model using Pressure Sensitive Paint (PSP) Technique," Journal of Visualization, **2**(1), 9–16.

Liu, T., B.T. Campbell, S.P. Burns, and J.P. Sullivan (1997), "Temperature- and Pressure-Sensitive Luminescent Paints in Aerodynamics," Applied Mechanics Reviews, **50**(4), 227-246

Liu, T., J.P. Sullivan (2005), Pressure and Temperature Sensitive Paints, Springer, New York, USA.

Sakaue, H. (1999), "Porous Pressure Sensitive Paints for Aerodynamic Applications," MS Thesis, School of Aeronautics and Astronautics, Purdue University, West Lafayette, IN.

Vukasinovic, B., D. Brzozowski, A. Glezer, W.W. Bower, and V. Kibens (2005), "Separation Control over a Surface-Mounted Hemispherical Shell," 35th AIAA Fluid Dynamics Conference and Exhibit (AIAA 2005-4878), Toronto, Ontario.